Cancer Chemother Pharmacol (1995) 35: 489–495

ORIGINAL ARTICLE

Bangaru Chandrasekaran · Timothy E. Kute
David S. Duch

Synchronization of cells in the S phase of the cell cycle by 3′-azido-3′-deoxythymidine: implications for cell cytotoxicity

Received: 4 April 1994/Accepted: 11 August 1994

Abstract The mechanism of synergy between 3′-azido-3′-deoxythymidine (AZT) and anticancer agents was investigated with emphasis on cell-cycle events. Exposure of exponentially growing WiDr human colon carcinoma cells to AZT resulted in synchronization of cells in the S phase of the cell cycle. Following treatment with AZT at 50 or 200 μ*M*, 62% ± 3% or 82% ± 4% of the cells were in the S phase as compared with 36% ± 2% in the control. Bromodeoxyuridine uptake studies revealed that the synchronized cells actively synthesized DNA. At concentrations of up to 200 μ*M*, AZT produced a cytostatic rather than cytotoxic effect as indicated by viability and cell growth measurements. At 200 μ*M*, AZT-induced synchronization was significant ($P = < 0.001$) after 12 h of drug exposure, reached a maximum at 24 h, and reversed to baseline levels by 72 h even in the continued presence of the drug. This indicates that AZT-induced cytostasis is a transient and reversible effect. The cell-cycle events seen with AZT in WiDr cells were also observed in eight of nine human tumor cell lines tested. Isobologram analysis of WiDr cells preexposed to AZT for 24 h and then exposed to either AZT-5-fluorouracil or AZT-methotrexate for a further 72 h revealed synergy between AZT and the anticancer agents, indicating that AZT-induced synchronization may have therapeutic benefits.

Key Words AZT · S-phase cytostasis · cytotoxicity · DNA histograms · 5-FU · MTX · flow cytometry

Abbreviations *AZT* · 3′-Azido-3′-deoxythymidine · *5-FU*, 5-fluorouracil · *MTX* methotrexate · *BrdUrd* bromodeoxyuridine · *MTT* 3-(4-5-dimethylthiazol-2-yl)-2,5-diphenyltetrazolium bromide

B. Chandrasekaran · D.S. Duch (✉)
Division of Cell Biology, Wellcome Research Laboratories, Research Triangle Park, NC 27709, USA

T.E. Kute
Department of Pathology, Bowman Gray School of Medicine, Winston-Salem, NC 27103, USA

Introduction

3′-Azido-3′-deoxythymidine (AZT, Retrovir) is active against human immunodeficiency virus [10,16] and is clinically used in patients with severe acquired immunodeficiency syndrome (AIDS)-related complex and AIDS [4,7,19]. AZT has been shown to act synergistically with the anticancer agents 5-fluorouracil (5-FU) and methotrexate (MTX) against human tumor cells [2,3,24,25]. The mechanism of action was postulated to be inhibition of thymidine kinase, since AZT is phosphorylated by this enzyme in cancer cells. As a result, AZT would be expected to block the synthesis of deoxythymidine triphosphate and should synergistically interact with inhibitors of deoxypyrimidine biosynthesis such as MTX and 5-FU, which are inhibitors of the thymidylate synthase cycle [24].

On the basis of studies in cisplatin-resistant cell lines, an additional role for AZT as an inhibitor of DNA repair and replication has also been postulated. Several studies led to the conclusion that cisplatin-resistant cells have an enhanced capacity to remove potentially lethal cisplatin-DNA adducts and resynthesize DNA in repair gaps [1,6,22]. The cisplatin-resistant cells overexpressed five enzymes (dihydrofolate reductase, thymidine kinase, thymidylate synthase, and DNA polymerases α and β) believed to be important for DNA replicative and repair synthesis [20]. These five enzymes are S-phase-specific enzymes and, moreover, DNA replicative and repair synthesis occurs in the S phase of the cell cycle. In earlier studies, inhibitors of DNA repair synthesis were shown to enhance the lethal effects of cisplatin [15,21]. The combination of AZT and cisplatin was 13 times more potent than an equivalent dose of cisplatin alone in cisplatin-resistant HCT-8 cells [20]. These observations led us to the

present investigation of changes in the cell-cycle events occurring in human tumor cells exposed to AZT.

In this study, we investigated AZT-induced cell-cycle perturbation and its relationship to cell growth and viability in human tumor cells. On the basis of these findings, we present a correlation between AZT-induced cell-cycle perturbation and synergistic cytotoxicity of combinations of AZT and 5-FU or AZT and MTX.

Materials and Methods

Chemicals and drugs

AZT and calcium leucovorin were supplied by Burroughs Wellcome Co. MTX and 5-FU were obtained from Sigma Chemical Co. Cell-culture medium was supplied by Gibco Laboratories, and fetal bovine serum was obtained from Hazelton Research Products, Inc. All other chemicals and reagents used were of analytical grade.

Cell culture

Human colon-carcinoma cell lines (WiDr, SW480, and SW620), a human melanoma cell line (A-375), a human pancreatic carcinoma cell line ($BxPC_3$), and a human breast carcinoma cell line (MCF-7) were obtained from the American Type Culture Collection (Rockville, Md.) The human leukemia cell line CCRF-CEM was provided by Dr. J. Bertino, Sloan Kettering Memorial Cancer Center (New York, NY.). The human colon carcinoma GC_3C_1 and its subline lacking thymidine kinase activity (GC_3/TK^-) were obtained from Dr.-J.-Houghton, St. Jude Hospital, (Memphis, Tenn.) [13]. The subline was selected with bromodeoxyuridine (Brdurd), was incapable growing in HAT medium, and was deficient in the cytosolic form of thymidine kinase. The WiDr, SW480, MCF-7, GC_3C_1, and GC_3C_1/TK^- cells were cultured in folate-free RPMI 1640 medium supplemented with 10 n*M* calcium leucovorin and 10% charcoal-dialyzed fetal bovine serum. All the remaining cell lines were cultured in RPMI 1640 medium supplemented with 10% fetal bovine serum. The cells were grown at 37°C in a humidified atmosphere containing 5% CO_2.

Growth inhibition (IC_{50} values) was determined using the MTT assay as described by Mossman [17]. Isobologram analysis was carried out as described previously [5].

DNA histogram and cell-cycle analysis

Exponentially growing human tumor cells were exposed to various concentrations of AZT and were harvested at different times using trypsin-ethylenediaminetetracetic acid (EDTA). The cells were fixed in ice-cold 70% ethanol (1 ml) and stored at 4°C for a minimum of 12 h but no longer than 1 week prior to further analysis. The cells were spun down at 1,000 *g* for 2 min and the supernatant was removed and discarded. The pellet containing cells (0.5–2-million) was stained for DNA with propidium iodide. In this procedure, the cell pellet was resuspended in 3.4-m*M* citrate buffer containing 0.01 *M* NaCl, 50 μg propidium iodide/ml, 0.6% NP-40, 37 μg RNAase/ml (75 Kunitz units/mg protein) at a pH of 7.6. Prior to analysis, the cells were passed through a 25-gauge needle and filtered through 40-μm mesh to remove any clumps. The cells were analyzed on a FACS STAR flow cytometer (Becton Dickinson FACS Systems) with excitation at 488 nm; the DNA fluorescence per cell was measured on a linear scale using a 630/22-nm bandpass filter. The list-mode data were collected for at least 20,000 particles using the Consort 30 program, and the DNA histogram data were analyzed using the MODFIT program (Verity Software). The determination of the distribution of cells in the G_1, S, and G_2 + M phases of the cell-cycle was based on a cell-size-gated population using defined markers for these parameters. There were at least duplicates for each analysis point, and the data given are mean values for the cell-cycle points.

BrdUrd incorporation as determined by flow cytometry

The cells exposed to AZT were further exposed to 8 μ*M* BrdUrd for 1 h at 37°C. The cells were spun at 1,000 *g* for 2 min and the supernatant was discarded. The cells were fixed with 70% ice-cold ethanol and stored at 4°C for a maximum of 1 week before further analysis. The pellet was washed with phosphate-buffered saline (PBS), treated with RNAse, acid-denatured, and treated with a fluorescein conjugate of anti-BrdUrd (Becton Dickinson Immuno Cytometry Systems) as described in the kit procedure. The DNA was then stained with 20 μ*g* propidium iodide/ml; the dual labeled cells were processed on a Becton Dickinson FACS STAR flow cytometer using excitation at 488-nm and measurement of log fluorescein isothiocyanate (FITC) incorporation per cell with a 530/30-nm bandpass filter. Controls for background fluorescence were carried out by elimination of addition of the primary antibody. The DNA fluorescence per cell was measured as described above. The two-color analysis was performed using the Consort 30 program.

Results

The results illustrated in Tables 1 and 2 confirm the findings obtained in other laboratories indicating that AZT interacts synergistically with both MTX and 5-FU. Treatment of WiDr cells for 24 h with AZT followed by further treatment for 72 h with the combination of AZT and MTX or AZT and 5-FU resulted in a synergistic inhibition of cell growth. AZT applied concurrently with or after the drugs exhibited additive effects. MTX and 5-FU are both cycle-specific antitumor drugs that are active in the S phase of the cell cycle. Moreover, although the IC_{50} of AZT in WiDr cells is high (approximately 100 μ*M*), this drug would also be expected to be active during the S phase. Thus, to determine whether the synergistic effects of AZT were related to changes in the cycling of the cells, we examined the effects of AZT on the cell cycle in WiDr cells.

Figure 1 illustrates changes in the cell-cycle distribution as determined by DNA staining with propidium iodide in WiDr cells treated with AZT at concentrations of 50 and 200 μ*M*. Treatment of the cells with AZT resulted in the accumulation of cells in the S phase. For the first 24 h of treatment with either concentration of AZT, there was a progressive accumulation of cells in the S phase with a corresponding decrease in the proportion of cells in G_1. Over the ensuing 48 h, there was cell division with an exit of cells from G_2 + M and reentry into G_1. Treatment of WiDr cells with AZT resulted in a significant increase ($P < 0.001$) in the percentage of cells in the S phase at

Table 1 Isobologram analysis of WiDr cells exposed to AZT and 5-FU[a]

Drugs (μM)	Validity	
	Observed	Predicted
AZT (100)	50.0	50
AZT (90) + 5-FU (0.18)	49.3	50
AZT (80) + 5-FU (0.36)	38.8	50
AZT (70) + 5-FU (0.54)	33.0	50
AZT (60) + 5-FU (0.72)	34.8	50
AZT (50) + 5-FU (0.9)	36.6	50
AZT (40) + 5-FU (1.08)	35.2	50
AZT (30) + 5-FU (1.26)	38.1	50
AZT (20) + 5-FU (1.44)	38.8	50
AZT (10) + 5-FU (1.62)	44.5	50
5-FU (1.8)	50.0	50

[a] A total of 2×10^3 cells were seeded in a 96-well microtiter plate, each well containing a volume of 150 µl. AZT was added 2 h later and 5-FU was added 24 h after AZT; the final volume was 300 µl. Under the experimental conditions the IC_{50} for 5-FU was 1.8 μM and that for AZT, 100 μM. The cells were incubated and processed, and viability was determined as described in Materials and methods. The results are mean values for a minimum of six data points

Table 2 Isobologram analysis of WiDr cells exposed to AZT and MTX[a]

Drugs (μM)	Validity	
	Observed	Predicted
AZT (100)	50.0	50
AZT (90) + MTX (0.0003)	45.5	50
AZT (80) + MTX (0.0006)	43.2	50
AZT (70) + MTX (0.0009)	40.8	50
AZT (60) + MTX (0.0012)	39.7	50
AZT (50) + MTX (0.0015)	34.8	50
AZT (40) + MTX (0.0018)	38.0	50
AZT (30) + MTX (0.0021)	40.6	50
AZT (20) + MTX (0.0024)	42.9	50
AZT (10) + MTX (0.0027)	46.1	50
MTX (0.003)	50.0	50

[a] Under the experimental conditions the IC_{50} for MTX was 0.003 μM and that for AZT, 100 μM. The cells were seeded and processed, and viability was determined as described in Table 2. AZT was added 24 h prior to MTX. The results are mean values for a minimum of six data points.

12 h after drug exposure, which at 24 h reached a maximum of 62% ± 3% and 82% ± 4% for AZT concentrations of 50 and 200 μM, respectively (Table 3). The percentage of cells in the S phase returned to baseline levels by 72 h, even in the continued presence of the drug. In controls, 36% + 2% of the cells accumulated in the S phase at 24 h.

Consistent with the cell-cycle effects, WiDr cells exposed to 50 μM AZT exhibited an increased division time during the first 24 h followed by growth resumption comparable with control values during the next 48 h. In the case of 200 μM AZT, there was no growth

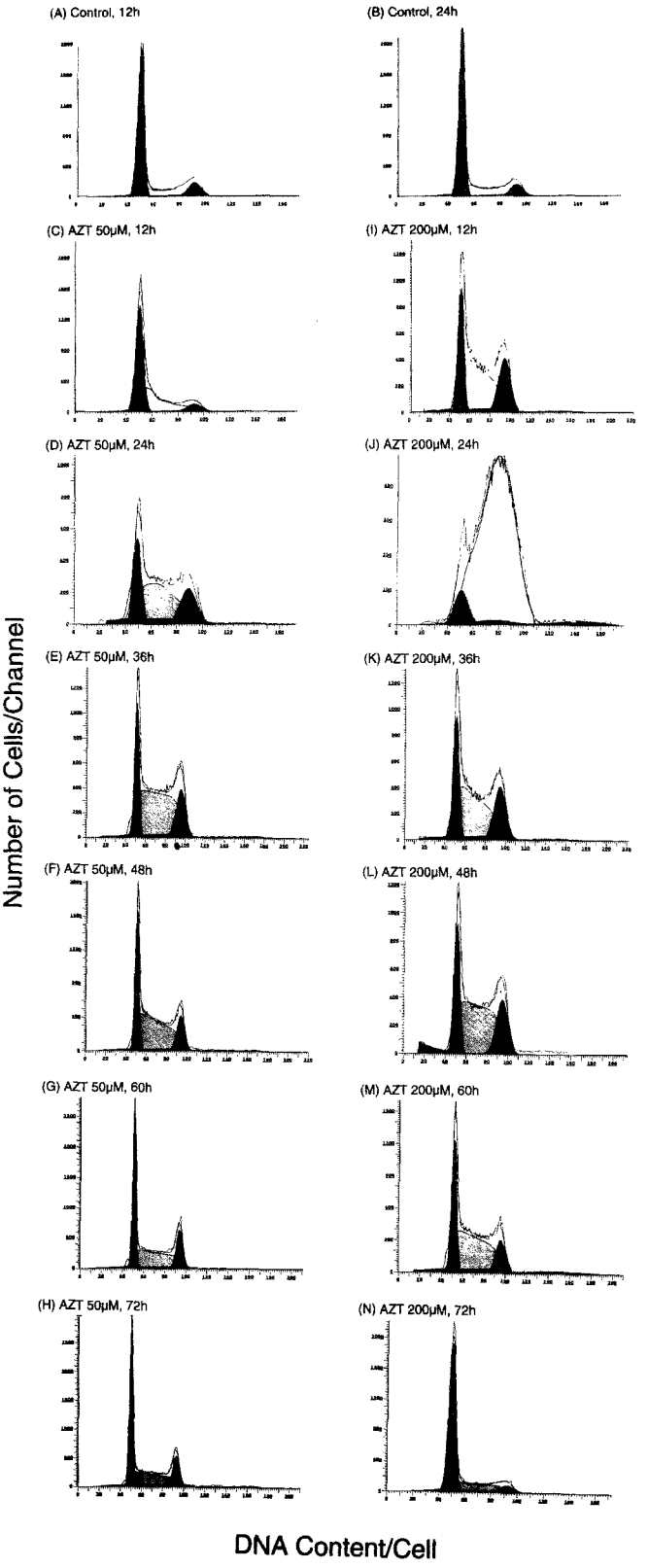

Fig. 1A–N DNA histograms of propidium iodide-stained WiDr cells. **A** controls at 12 h. **B** controls at 24 h. **C–H** Cells treated with 50 μM AZT for 12–72 h and **I–N** cells treated with 200 μM AZT for 12–72 h as described in Materials and methods. The peak visible at channel number 50 is G_1 and that visible at channel number 90–95 is G_2/M

Table 3 DNA historgrams of propidium iodide-stained WiDr cells exposed to AZT[a]

Drug	% Cells in		
	G_1	S	$G_2 + M$
Control, 12 h	46	36	18
AZT, 50 μ*M*, 12 h	37	55	8
AZT, 200 μ*M*, 12 h	34	61	5
control, 24 h	47	36	17
AZT, 50 μ*M*, 24 h	30	62	8
AZT, 200 μ*M*	14	82	4
Control, 36 h	40	40	20
AZT, 50 μ*M*, 36 h	26	53	21
AZT, 200 μ*M*, 36 h	17	61	22
Control, 48 h	44	37	19
AZT, 50 μ*M*, 48 h	25	54	21
AZT 200 μ*M*, 48 h	20	62	18
Control, 60 h	48	37	15
AZT 50 μ*M*, 60 h	35	48	17
AZT 200 μ*M*, 60 h	37	48	15
Control, 72 h	48	36	16
AZT 50 μ*M*, 72 h	41	44	15
AZT 200 μ*M*, 72 h	40	43	17

[a] The numbers were generated using MODFIT analysis

in the first 24 h, which was consistent with an almost total block of the cells in the S phase (Fig. 1). Growth retardation occurred during the next 24 h, which was followed by a return to control growth rates within 72 h, even in the continued presence of the drug. Trypan blue dye exclusion showed a viability of 95% at all time points (Table 4). The AZT-induced cell-cycle perturbations were time- and concentration-dependent over a concentration range of 3–200 μ*M*. There was no cell-cycle perturbation effect during the first 5 h of AZT exposure. AZT-induced cell-cycle perturbations were maximal at 12–24 h after drug addition and then returned to baseline levels, even in the presence of the drug. The cell-cycle effects observed with AZT in WiDr cells were also observed in colon carcinomas SW480 and SW620, MCF-7 breast carcinoma, BxPC3 pancreatic carcinoma, A375 melanoma, and CCRF-CEM leukemia (Table 5). The results illustrated in Table 6 indicate that phosphorylation of AZT is required for synchronization of cells. GC_3TK^- cells, which lack the enzyme thymidine kinase and, thus, the ability to phosphorylate AZT to the monophosphate, do not exhibit synchronization in the presence of AZT. In contrast, treatment of the parent line from which this clone was derived (GC_3C_1) with 200 μ*M* AZT led to the accumulation of approximately 90% of the cells in the S phase at 24 h.

BrdUrd uptake studies using a fluorescein conjugate of an antibody to BrdUrd (Table 7) showed that the cells blocked in the S phase by AZT actively synthesized DNA and that less than 3% of the AZT-treated cells were in the dormant SO stage. This further confirms that exposure of exponentially growing WiDr cells to AZT at concentrations of up to 200 μ*M* for 72 h is not cytotoxic.

Discussion

In this report, we describe a novel mechanism by which AZT can produce a synergistic interaction with S-phase-specific anticancer agents. AZT caused a time and concentration-dependent synchronization of human tumor cells in the S phase of the cell cycle. This synchronization was dose-dependent, transient, reversible, and cytostatic in nature. AZT at 200 μ*M* produced an almost total arrest of cells in the S phase of the cell cycle, whereas at lower concentrations, transit through the cell cycle was slowed significantly, though not completely. Synchronization parallels and may be related to the decreases in deoxynucleotides observed following treatment of cells with AZT [8,9]. These studies [8,9] showed that treatment with 200 μ*M* AZT resulted in decreased levels of deoxythymidine triphosphate (dTTP) and deoxyguanosine triphosphate (dGTP), which returned to near normal levels by 24 h. When cells are treated with AZT, the transient decrease in dTTP occurs at the same time as an increase in the levels of AZT and its phosphorylated derivatives, including AZT triphosphate (AZTTP). Since AZT and thymidine compete for the same enzymes (i.e., thymidine kinase, thymidylate kinase, and DNA polymerase), decreased levels of dTTP would allow for the increased incorporation of AZTTP into DNA. As dTTP levels again increase, there would be increased incorporation of dTTP into DNA relative to AZTTP due to the more favorable kinetic parameters of thymidine and dTTP for the synthetic enzymes. This

Table 4 Growth rates of WiDr cells proposed to AZT

Drug	Doubling time (h)				% Viability[a]		
	0–24	24–48	48–72	0–72	24 h	48 h	72 h
Control	19.6	21.6	23.6	21.7	100	100	98
AZT, 50 μ*M*	90.6	19.5	23.6	27.7	100	100	97
AZT, 200 μ*M*	NG	41.4	22.0	48.0	98	100	98

[a] Viability was assessed using trypan blue dye exclusion
(*NG*, no growth)

Table 5 Cell-cycle distribution in human tumor cells exposed to AZT[a]

	% Cells in		
	G_1	S	$G_2 + M$
CCRF-CEM:			
Control, 12 h	16	54	30
AZT, 50 μ*M*, 12 h	30	55	15
AZT, 200 μ*M*, 12 h	0	65	35
Control, 24 h	40	45	15
AZT, 50 μ*M*, 24 h	27	68	5
AZT, 200 μ*M*, 24 h	0	89	11
SW-480:			
Control, 12 h	40	46	14
AZT, 50 μ*M*, 12 h	25	70	5
AZT, 200 μ*M*, 12 h	13	87	0
Control, 24 h	39	48	13
AZT, 50 μ*M*, 24 h	34	52	14
AZT, 200 μ*M*, 24 h	22	69	9
SW-620:			
Control, 12 h	40	45	15
AZT, 50 μ*M*, 12 h	27	68	5
AZT, 200 μ*M*, 12 h	23	73	4
Control, 24 h	38	45	17
AZT, 50 μ*M*, 24 h	20	65	15
AZT, 200 μ*M*, 24 h	12	88	0
MCF-7:			
Control, 12 h	56	22	22
AZT, 50 μ*M*, 12 h	46	47	7
AZT, 200 μ*M*, 12 h	53	39	8
Control, 24 h	52	28	20
AZT, 50 μ*M*, 24 hz	41	57	2
AZT, 200 μ*M*, 24 h	49	49	2
BxPC3:			
Control, 12 h	63	16	21
AZT, 50 μ*M*, 12 h	52	38	10
AZT, 200 μ*M*, 12 h	55	40	5
Control, 24 h	44	34	22
AZT, 50 μ*M*, 12 h	16	78	6
AZT, 200 μ*M*, 12 h	7	93	0
A375:			
Control, 12 h	15	55	30
AZT, 50 μ*M*, 12 h	2	74	24
AZT, 200 μ*M*, 12 h	0	79	21
Control, 24 h	17	54	29
AZT, 50 μ*M*, 24 h	11	64	25
AZT, 200 μ*M*, 24 h	0	94	6

[a] Cells exposed to AZT were fixed in ice-cold 70% ethanol and kept in a refrigerator for a minimum of 12 h (but no more than a week) until analysis by flow cytometry as described in Materials and methods

Table 6 Role of thymidine kinase in synchronization of cells by AZT

	% Cells in		
Cell/treatment	G_1	S	$G_2 + M$
GC3C1:			
Control, 12 h	36	42	22
AZT, 50 μ*M*, 12 h	37	40	23
AZT, 200 μ*M*, 12 h	43	40	17
Control, 24 h	47	32	21
AZT, 50 μ*M*, 24 h	11	78	11
AZT, 200 μ*M*, 24 h	6	91	3
GC3/TK$^-$:			
Control, 12 h	49	33	18
AZT, 50 μ*M*, 12 h	52	25	23
AZT, 200 μ*M*, 12 h	52	24	24
Control, 24 h	49	32	19
AZT, 50 μ*M*, 24 h	48	27	25
AZT, 200 μ*M*, 24 h	45	34	21

Table 7 BrdUrd uptake studies in WiDr cells exposed to AZT

	% Cells in				
	G_1	S			$G_2 + M$
		ES	LS	SO	
Control, 24 h	27	19	57: 35	3	16
AZT, 50 μ*M*, 24 h	18	16	66: 45	5	16
AZT, 200 μ*M*, 24 h	10	30	84: 50	4	6
Control, 72 h	31	18	51: 30	3	18
AZT, 50 μ*M*, 72 h	27	13	52: 39	3	21
AZT, 200 μ*M*, 72 h	22	14	60: 46	0	18

return corresponded to the time in these studies at which the cell-cycle distribution began to reverse toward normal.

The ability of AZT to induce synchronization appeared to be dependent on phosphorylation of the nucleoside. Treatment of GC3TK$^-$, a cell line deficient in thymidine kinase, the enzyme responsible for the phosphorylation of AZT, had no effect on the cell-cycle distribution in this cell line. Moreover, preliminary studies have indicated that the extent of the S phase block correlates with the amount of AZT incorporated into DNA (D.Duch, unpublished data). It had previously been shown [9] that AZT could synchronize the leukemic cell line CCRF-CEM in the S phase of the cell cycle. The results of this study show that AZT can also effectively synchronize cells derived from solid tumors.

Recently, Keyomarsi et al. [14] described an effective procedure for the synchronization of tumor cells using lovastatin. This procedure arrested mammalian cells in the G_1 phase of the cell cycle but required a second agent, mevalonic acid, to reverse the synchrony. In contrast, AZT-induced synchronization is reversible without addition of a second agent, even in the

continued presence of the drug. AZT treatment did not result in cell killing as determined by viability and cell growth measurements. BrdUrd uptake studies revealed that the arrested cells actively synthesized DNA, indicating the cytostatic nature of the AZT-induced cell-cycle effect. One approach to optimization of therapy is based on observations that the cell-cycle-traversing properties of malignant tumors and therapy-limiting host tissues are often distinctly different and that a variety of anticancer agents exist that kill or block cells only in limited parts of the cell cycle [11]. Cytokinetic strategies are based on observations that the tumor and/or normal cells can be partially synchronized during therapy and that the administration of cell-cycle-specific cytotoxic agents can be timed to maximize tumor-cell killing and/or to minimize normal-cell killing. These results suggest that pretreatment with AZT may modulate the tumor cells favorably to increase the therapeutic index of the anticancer agent.

Pretreatment of WiDr cells for 24 h with AZT followed by the combination of AZT and 5-FU or AZT and MTX resulted in synergistic cell-growth inhibition. Both 5-FU and MTX are S-phase-specific anticancer agents. The synergistic cytotoxicity seen in this study may have been due to synchronization of cells in the S phase of the cell cycle induced by AZT due to pretreatment followed by lysis of those cells in the S phase by the S-phase-specific cytotoxic agents 5-FU and MTX. Other mechanisms for the mode of action of AZT have been proposed. Weber et al. [24,25] proposed that through its inhibition of thymidine salvage, AZT synergistically enhanced the antitumor effects of MTX and 5-FU, both inhibitors of de novo thymidylate biosynthesis. Although inefficient as a substrate for cellular DNA polymerases, AZT can be incorporated into DNA and, when incorporated, acts as a chain terminator [18,23]. AZT that has been incorporated into DNA can be removed by a 3′-exonuclease activity, although the repair process may be saturated at high levels of AZT. Harrington et al. [12] have shown that AZT monophosphate is an inhibitor of 3′exonuclease purified from two different human cell lines and that the high levels of AZT monophosphate present following AZT treatment may be sufficient to inhibit the exonuclease activity and, hence, DNA repair. Indeed, Scanlon et al. [20,21] have proposed that AZT potentiates the antitumor activity of cisplatin through its effects on DNA repair.

In summary, we report a novel mechanism of synchronization of human tumor cells by AZT leading to synergistic interaction with S-phase-specific agents. This warrants further investigation in vitro and in vivo.

References

1. Ahnstrom G (1989) Inhibition of DNA strand break rejoining in ultraviolet-irradiated human cells: comparision of aphidicolin and cytosine arabinoside. Biochim Biophys Acta 1007: 357–358
2. Brunetti I, Darnowski JW, Falcone A, Johnson KA, Calabresi P (1989) Azidothymidine enhances fluorouracil and methotrexate antitumor and therapeutic activity. Proc Am Assoc Cancer Res 30: 595
3. Brunetti I, Falcone A, Calabresi P, Goulette FA, Darnowski JW (1990) 5-Fluorouracil enhances azidothymidine cytotoxicity: In vitro, in vivo, and biochemical studies. Cancer Res 50: 4026–4031
4. Chaisson RE, Allain J-P, Leuther M, Volberding PA (1986) Significant changes in HIV antigen level in the serum of patients treated with azidothymidine. N Engl J Med 315: 1610–1611
5. Chou T, Talay P (1984) Quantitative analysis of dose-effect relationships: the combined effects of multiple drugs or enzyme inhibitors. Adv Enzyme Regul 22: 27–55
6. Eastman A, Schulte N (1988) Enhanced DNA repair as a mechanism of resistance to *cis*-diamminedichloroplatinum (II). Biochemistry 27: 4730–4734
7. Fischl MA, Richman DD, Grieco MH, Gottlieb MS, Volberding PA, Laskin OL, Leedom JM, Groopman JE, Mildvan D, Schooley RT, Jackson GG, Durack DT, King D, the AZT Colloborative Working Group (1987) The efficacy of azidothymidine (AZT) in the treatment of patients with AIDS and AIDS-related complex: a double-blind, placebo-controlled trial. N Engl J Med 317: 185–191
8. Frick LW, Nelson DJ, St Clair MH, Furman PA, Krenitsky TA (1988) Effect of 3′-azido-3′-deoxythymidine on the deoxynucleotide triphosphate pools of cultured human cells. Biochem Biophys Res Commun 154: 124–129
9. Fridland A, Connelly MC, Ashmun R (1990) Relationship of deoxynucleotide changes to inhibition of DNA synthesis induced by the antiretroviral agent 3′-azido-3′-deoxythymidine and release of its monophosphate by human lymphoid cells (CCRF-CEM). Mol Pharmacol 37: 665–670
10. Furman PA, Fyfe JA, St Clair MH,Weinhold K, Rideout JL, Freeman GA, Nusinoff-Lehrmann S, Bolognesi DP, Broder S, Mitsuya H, Barry DW (1986) 3′-Azido-3′-deoxythymidine and selective interaction of the 5′-triphosphate with human immunodeficiency virus reverse transcriptase. Proc Natl Acad Sci USA 83: 8333–8337
11. Gray JW, Pallavicini MG (1982) Ara-C scheduling: theoretical and experimental considerations. Med Pediatr Oncol 10 [suppl 1]: 93–108
12. Harrington JA, Reardon JE, Spector T (1993) 3′-Azido-3′-deoxythymidine (AZT) monophosphate: an inhibitor of exonucleolytic repair of AZT-terminated DNA. Antimicrob Agents Chemother 37: 918–920
13. Houghton PJ, Houghton JA, Germain G, Torrance PM (1987) Development and characterization of a human colon adenocarcinoma xenograft deficient in thymidine salvage. Cancer Res 47: 2117–2122
14. Keyomarsi K, Sandoval L, Band V, Pardee AB (1991) Synchronization of tumor and normal cells from G_1 to multiple cell cycles by lovastatin. Cancer Res 51: 3602–3609
15. Lai G-M, Ozols RF, Smyth JF, Young RC, Hamilton TC (1988) Enhanced DNA repair and resistance to cisplatin in human ovarian cancer. Biochem Pharmacol 37: 4597–4600
16. Mitsuya H,Weinhold KJ, Furman PA, St Clair MH, Nusinoff-Lehrman S, Gallo RC, Bolognesi D, Barry DW, Broder S (1985) 3′-Azido-3′-deoxythymidine (BW A509 U): an antiviral agent that inhibits the infectivity and cytopathic effect on human T-lymphotropic virus type 111/lymphadenopathy-associated virus in vitro. Proc Natl Acad Sci USA 82: 7096–7100
17. Mossmann T (1983) Rapid colorimetric assay for cellular growth and survival: application to proliferation and cytotoxicity assays. J Immunol Methods 65: 55–63

18. Nickel W, Austermann S, Bialek G, Grosse F (1992) Interactions of azidothymidine triphosphate with the cellular DNA polymerases α, δ, and ε and with DNA primase. J Biol Chem 267: 848–854
19. Richman DD, Fischl MA, Grieco MH, Gottlieb MS, Volberding PA, Laskin OL, Leedom JM, Groopman JE, Mildvan D, Hirsch MS, Jackson GG, Durack DT, Nusinoff-Lehrman S, the AZT Colloborative Working Group (1978) the toxicity of azidothymidine (AZT) in the treatment of patients with AIDS and AIDS-related complex. N Engl J Med 317: 192–197
20. Scanlon KJ, Kashani-Sabet M, Sowers LC (1989) Overexpression of DNA replication and repair enzymes in *cis*platin-resistant human colon carcinoma HCT8 cells and circumvention by azidothymidine. Cancer Commun 1: 269–275
21. Scanlon KJ, Funato T, Pezeshki B, Tone T, Sowers LC (1990) Potentiation of azidothymidine cytotoxicity in *cis*platin-resistant human ovarian carcinoma cells. Cancer Commun 2: 339–343
22. Swinnen LJ, Barnes DM, Fisher SG, Albain KS, Fisher RI, Erickson LC (1989) 1-β-D-Arabinofuranosylcytosine and hydroxyurea production of cytotoxic synergy with *cis*-diamminedichloroplatinum(II) and modification of platinum-induced DNA interstrand cross-linking. Cancer Res 49: 1383–1389
23. Vazquez-Padua MA, Starnes MC, Cheng Y-C (1990) Incorporation of 3′-azido-3′-deoxythymidine into cellular DNA and its removal in a human leukemic cell line. Cancer Comm 2: 55–62
24. Weber G, Ichikawa S, Nagai M, Natsumeda Y (1990) Azidothymidine inhibition of thymidine kinase and synergistic cytotoxicity with methotrexate and 5-fluorouracil in rat hepatoma and human colon cancer cells. Cancer Commun 2: 129–133
25. Weber G, Nagai M, Prajda N, Nakamura H, Szekeres T, Olah E (1991) AZT: a biochemical response modifier of methotrexate and 5-fluorouracil cytotoxicity in human ovarian and pancreatic carcinoma cells. Cancer Commun 3: 127–132